Gleissberg Cycle Dependence of Inner Zone Proton Flux

Emily J. Bregou[1, 2], Mary K. Hudson[1, 3], Brian T. Kress[4], Murong Qin[5], and Richard S. Selesnick[6]

[1] NCAR *High Altitude Observatory, Boulder, CO, USA*
[2] *Dept. of Physics and Astronomy, University of Pennsylvania, Philadelphia, PA, USA*
[3] *Physics and Astronomy Dept., Dartmouth College, Hanover, NH, USA*
[4] *Center for Cooperative Research in the Environmental Sciences at CU Boulder, Boulder, CO, USA*
[5] *Center for Space Physics, Boston University, Boston, MA, USA*
[6] *Space Vehicles Directorate, Air Force Research Laboratory, Kirtland AFB, NM, USA*

Corresponding author: Emily Bregou (ebregou@sas.upenn.edu)

Key Points:

- **POES MeV proton measurements from 1980-2021 are anticorrelated with F10.7**
- **Observations are consistent with model prediction of a long term proton flux increase**
- **Centennial Gleissberg Cycle solar minimum impact on inner zone proton flux is found.**

Plain Language Summary

The inner zone proton radiation belt consisting of 10's to >100 MeV protons trapped in the Earth's magnetic field is examined from 1980 to mid-2021 using measurements from four NOAA POES satellites. A long-term increase in measured proton flux over four ~11 year cycles of solar activity is found. This increase correlates with the current one hundred year minimum in solar activity known as the Gleissberg cycle. Inner zone proton flux is correlated with decreasing solar irradiance maxima at a wavelength of 10.7 cm, serving as proxy for Extreme Ultra Violet input to Earth's atmosphere. It is found that current peak proton flux, occurring at a longitude and latitude where the Earth's magnetic field is weaker, is at the highest levels seen since 1980. A model calculation of the inner zone proton flux is found to generally confirm the long-term trend. We conclude that this trend observed over ~ 40 years accompanies an average decrease in solar EUV. The reduced EUV at solar maximum reduces proton loss to the atmosphere, thus explaining the observed long-term increase in inner zone proton flux.

Abstract

Inner zone proton flux from 1980 to mid-2021is examined using NOAA POES satellite data, indicating a long-term increase corresponding to a one hundred year minimum in solar activity

consistent with the Centennial Gleissberg Cycle. Variation of inner belt protons is correlated with decreasing F10.7 maxima over the 40-year period, serving as proxy for solar EUV input to Earth's atmosphere. Extending an earlier study (Qin et al., 2014) of > 70 MeV protons from 1980 – 2021 using the South Atlantic Anomaly (SAA) peak flux, and at fixed L = 1.3, a comparison is made between the > 35, > 70 and > 140 MeV energy channels on POES. All three energies show an increase in proton flux over the period 1998 – 2021 using a single spacecraft. The observed flux increase is correlated with decreasing F10.7 over the longer 40-year time interval, as with the ~11-year solar cycle. A phase lag during Solar Cycle 24 (January 2010 – June 2021) between the F10.7 minimum and proton flux maximum was determined to be ~500 days, the same at all energies studied. A model calculation of the inner zone proton flux is found to generally confirm the long-term trend examined both in absolute magnitude and phase lag. It is concluded that this long-term trend is a manifestation of the concurrent Gleissberg cycle minimum and accompanying decrease in solar EUV. Reduced EUV at solar maximum (F10.7proxy) reduces proton loss to the atmosphere following solar maximum, thus explaining the long-term flux increase observed.

1 Introduction

The Earth's inner radiation belt, the first discovery of the Space Age (Van Allen et al., 1958), consists of high energy protons (10 MeV–1 GeV) and lower energy electrons trapped in the Earth's magnetic field. The sources of inner belt protons, the focus of this paper, include Cosmic Ray Albedo Neutron Decay (CRAND) and Solar Energetic Protons (Selesnick, Hudson, & Kress, 2010; Selesnick, Looper, & Mewaldt, 2007). The very energetic proton population, while constrained to an altitude below ~10^4 km, is a known hazard to low and medium altitude satellites (Stassinopoulos and Raymond, 1988; Dyer, 2002) and to the International Space Station whose orbit encounters the South Atlantic Anomaly. The South Atlantic Anomaly (SAA) is a region where the inner zone proton flux is observed to increase at low altitude. This is due to a weakening in the Earth's magnetic field presently spanning a range at 500 km altitude of -90 to +40 degrees in geographic longitude and -50 to 0 degrees in geographic latitude. This region of weaker magnetic field, which is slowly decreasing in time (Pavón-Carrasco & De Santis, 2016), allows inner zone protons to mirror closer to Earth.

The proton flux in the inner zone is anticorrelated with solar activity (Nakagano and Heckman, 1968; Dragt, 1971; Huston et al., 1998; Kuznetsov et al., 2010; Qin et al., 2014; Li et al., 2020; Lin et al., 2020). During solar maximum, the upper atmosphere is heated and expands due to increased solar EUV (Gombosi, 1998), so protons encounter higher neutral density along their trajectories. In addition, photoionization and increased auroral activity increase ionospheric density (Gombosi, 1998). The inner zone protons lose energy primarily via Coulomb collisions with both free and bound electrons (Selesnick et al., 2007; Selesnick and Albert, 2019), thus explaining the lower flux levels observed above a fixed energy following solar maximum. There is a lag between solar maximum and proton flux minimum due to the time scale for proton energy loss (Qin et al., 2014; Li et al. 2020, Lin et al., 2020). This effect on inner zone proton loss dominates the solar cycle modulation of Galactic Cosmic Rays which provides the CRAND source of inner zone protons and is also anticorrelated with the solar cycle (Li et al., 2020).

Previous studies have examined the solar cycle variation using different energy channels of the SEM-1 and SEM-2 instruments (Rabin et al., 1995; Evans and Greer, 2006) on the NOAA Polar

Operational Environment Satellites (POES) in sun synchronous polar orbits at approximately 850 km, also used for this study. Qin et al. (2014) examined solar cycle modulation of the > 70 MeV proton flux from POES measurements for the period from 1980 through 2009. Li et al. (2020) examined the > 36 MeV and > 140 MeV proton flux measured by a single POES (NOAA-18) satellite over the shorter time interval from 2005 – 2018, also examining the SAMPEX PET differential proton flux measurements (Cook et al., 1993) at 27.4 – 37.4 MeV over the period 1992 – 2009. The polar orbiting (82 degree inclination) SAMPEX measurements were made at an altitude of approximately 500 km (±20 km) and L = 1.33–1.42. Li et al. (2020) found a solar cycle modulation in the SAMPEX PET measurements at 500 km altitude of 300% while at the higher altitude of POES measurements they found a solar cycle modulation of 21%. Lin et al. (2020) recalibrated data from the >16-MeV proton integral fluxes obtained from NOAA POES and EUMETSAT MetOp satellites, also carrying the SEM-2 instrument, from the period 1978 to 2014, examining solar cycle phase lags and the relationship between trapped proton fluxes and F10.7. They focused on measurements at L = 1.2, below the energy-dependent inner zone flux peak (Ginet et al., 2013), and found no long term increase in flux at this L value for > 16 MeV protons.

This paper examines data spanning a period from 1980 to the present day to illustrate a long-term trend of increasing proton flux in the inner zone from the POES data set that corresponds to a one hundred year minimum in solar activity. Prior studies can now be extended beyond the most recent solar minimum 2018-2019, capturing the trapped proton flux increase to the highest levels seen since 1980. This longer term data set allows us to investigate the Gleissberg cycle variation of inner belt protons (Gleissberg, 1965). First, the study by Qin et al. (2014) of > 70 MeV proton flux from 1980 through 2009 is extended through June 2021, using their method for determining peak flux in the SAA, then comparing with > 70 MeV flux at fixed L = 1.3. A comparison is then made between the > 35, > 70 and > 140 MeV energy channels on POES. The phase lag during Solar Cycle 24 (January 2010 – June 2021) between F10.7 and proton flux for these three energy channels is then determined. A model calculation of the inner zone proton flux based on Selesnick et al. (2007) is then presented which confirms the long term trend examined here. Finally, discussion and conclusions are presented in the context of the Centennial Gleissberg Cycle minimum in solar activity (Gleissberg, 1965; Feynmann and Ruzmaikin, 2011; Pulkinnen et al., 2001) and its effect on the long term trend seen in inner zone proton flux.

2 POES Data

The data in this study come from the POES satellites which are low altitude polar orbiting satellites launched by NOAA since 1978. The POES proton data were accessed for four consecutive POES satellites: NOAA-06 (January 1st, 1980 - August 18th, 1986), NOAA-10 (October 11th, 1986 - January 27th 1991), NOAA-12 (January 1st 1992 - March 1st 2002), and NOAA-15 (January 1st 1999 - present day). Proton counts come from an instrument on board called the Space Environment Monitor or SEM with the original SEM-1 instrument aboard the NOAA-06, NOAA-10, and NOAA-12 satellites and the upgraded SEM-2 aboard NOAA-15 (https://www.ngdc.noaa.gov/stp/satellite/poes/). The Space Environmental Monitors host a variety of detectors to measure energetic electrons and ions (Evans and Greer, 2006). Omnidirectional proton counts per second used in this application come from the medium energy proton and electron detector or MEPED. This consists of a solid state detector located under a

hemisphere of tungsten, the thickness of which sets energy detection thresholds. To convert counts per second to omnidirectional integral flux, we calculated a conversion factor of 2.9 cm^{-2}. We used the detector front and back area of 0.5 cm^2 and side area of 0.752 cm^2 (Evans and Greer, 2006) and assumed that the detector axis was aligned with the magnetic field. In the absence of pitch angle information from the POES satellite, we assumed an isotropic proton flux outside the drift loss cone and zero flux inside. We expect the actual flux to peak at 90 degrees (Selesnick et al., 2014) which, if accounted for, would result in slightly higher measured flux.

Solar proton events or SPEs occur when particles emitted from the sun are accelerated, either in solar flares or by interplanetary shocks produced by Coronal Mass Ejections (CMEs). Proton flux is seen to increase suddenly during SPE events produced by solar flares and more gradually from CME shocks (Reames et al., 1999). Since this study focuses on long term trends, changes in the proton population that occur over shorter timescales must be removed. Protons with energies in the 10s of MeV are known to be present at high latitudes (high L-values) during SPEs but not during solar quiet times. As such, all data corresponding to time periods in which there is a high flux of 16 MeV protons at high latitude have been removed from the dataset (Qin et al., 2014).

3 Observational Results

Figure 1 is a plot of the peak flux of >70 MeV protons in the SAA from 1980 to 2021. Following the technique employed by Qin et al. (2014), we divided data into bins of 3 months. We then selected a longitudinal range of 6° corresponding to the highest flux in the SAA. A different longitudinal range was used for each of the four POES spacecraft to account for the slowly changing position of the SAA. We then fit a Gaussian in latitude to estimate the value of the peak flux. The data are normalized to one at the beginning of 2010 to facilitate comparison to Figure 3 appearing in Qin et al. (2014). F10.7 cm flux, representing solar activity, is included for comparison.

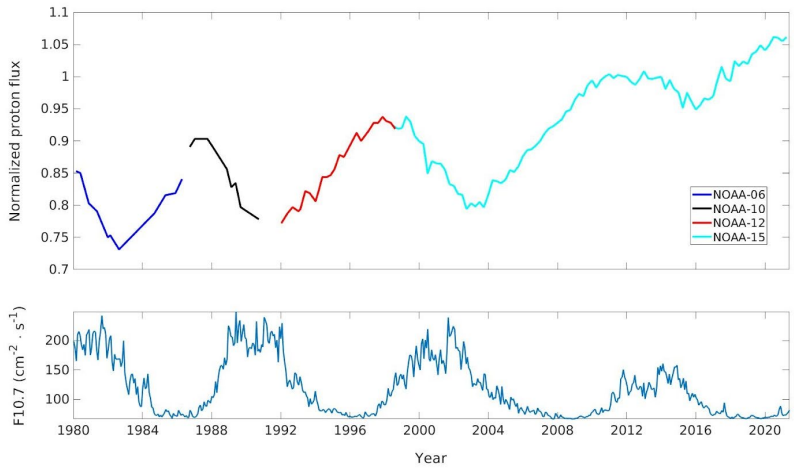

Figure 1. 3-month averaged peak flux for >70 MeV protons in the SAA is normalized to flux (= 1) at the beginning of 2010 (top) and plotted against 10.7cm solar flux (F10.7, bottom) from 1980 to June, 2021 to extend Figure 3 in Qin et al. (2014) which covered 1980 through 2009. Different colors are used to represent different POES satellites. Prior to the NOAA-15 data

beginning in 1999, satllites measured >80 MeV proton flux. Qin et al. (2014) found good agreement between the >80 MeV and >70 MeV proton flux data and determined that no correction factor was necessary.

The proton flux increases over this more than forty year time span by a factor of 1.2. It is also evident in **Figure 1** that the intensity of solar maxima as measured by F10.7 weakens over time. Superimposed on the long term trend is the solar cycle variation of both proton flux and F10.7, with a phase lag in the peak proton flux following solar minimum reported previously (Qin et al., 2014; Li et al., 2020; Lin et al., 2020) and examined further below. The magnitude of the F10.7 variation is greater than the solar cycle variation of galactic cosmic rays (>GeV) with peak flux at solar minimum, providing a source for these trapped protons through the CRAND process (Singer et al., 1958; Li et al., 2020). This leads to the conclusion that change in atmospheric and ionospheric density with the solar cycle variation in EUV flux affects proton energy loss (Selesnick et al., 2007) and is ultimately responsible for both the solar cycle variation (Qin et al., 2014; Li et al., 2020; Lin et al., 2020) and long term trend reported here.

In **Figure 1**, we plot the maximum flux in the SAA for >70 MeV protons found using a Gaussian (independent of L-value) fit to the maximum flux. In **Figure 2**, we plot a comparison between >70 MeV proton flux at constant L = 1.3 in the SAA and the maximum flux from 1998 to 2021. The same trends are observed for both methodologies.

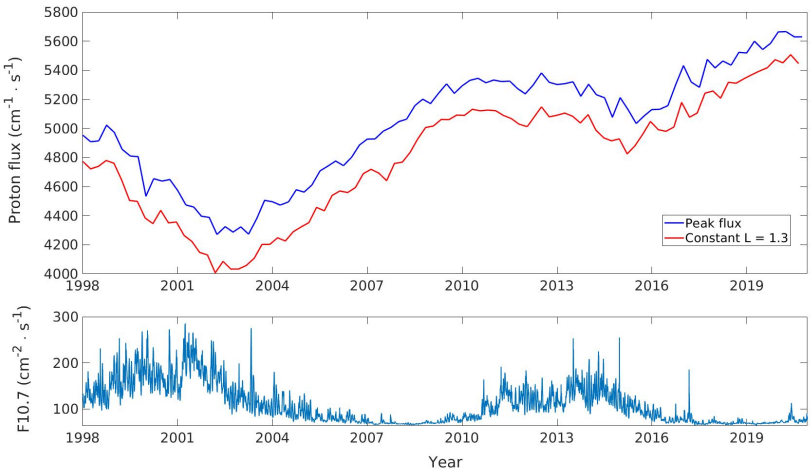

Figure 2. (Top) >70 MeV flux at constant L = 1.3 in the SAA (blue) from January, 1998 to June, 2021 compared with peak flux (red) from Figure 1; (Bottom) F10.7.

Figure 3 demonstrates that the flux increase is visible across multiple energy channels. The Solar Cycle 24 flux minimum was found to be 19% higher (averaged over energy channels) than the Solar Cycle 23 minimum. The peak flux plotted here for >35 MeV and >140 MeV protons was determined using the same Gaussian method as was used for >70 MeV protons in **Figures 1** and **2**.

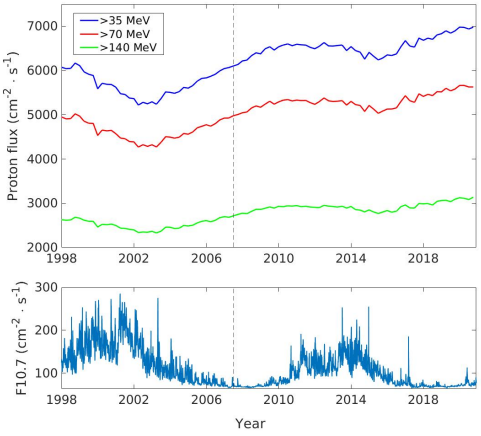

Figure 3. (Top) 3-month averaged peak flux in the SAA for >35, >70, and >140 MeV protons. A dashed line is added to indicate the change from Solar Cycle 23 to Solar Cycle 24 in 2008; (Bottom) F10.7.

We also calculated the phase lag between F10.7 and proton flux for Solar Cycle 24 for the same three energy channels that are shown in **Figure 3**. **Figure 4** shows the correlation coefficient for different phase lag values. We obtain the best fit at 510 days for all three energy channels with a correlation coefficient of 0.73. Qin et al., (2014) previously calculated the phase lag to be 705 days, 380 days, and 685 days for Solar Cycles 21, 22, and 23 respectively and did not find any dependence on proton energy. Li et al., (2020) estimated proton flux from POES satellites and sunspot number using a sine function with 11-year period and estimated a phase lag of 730 days for 2005-2015. They calculated phase lag for >36 MeV and >140 MeV protons, however, the energy dependence for phase lag was not analyzed.

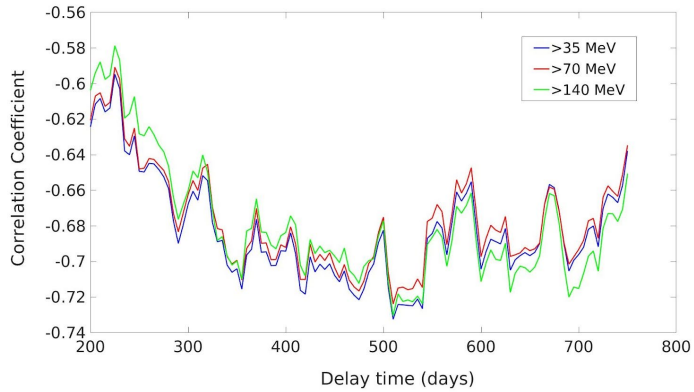

Figure 4. Anticorrelation between peak proton flux in the SAA and F10.7 flux is plotted as a function of time lag for three energy channels for Solar Cycle 24 (January, 2010 - June, 2021).

4 Model Comparison

To provide additional insight into the causes of observed variation in the SAA proton flux, theoretical predictions have been made with the proton radiation belt model of Selesnick et al. (2007), as updated by Selesnick and Albert (2019). Model results showing the maximum omnidirectional integral (>70 MeV) proton flux in the SAA region at POES altitude, as a function of time since 1980, are shown in Figure 5, for comparison to the observations in Figure 1. The trend of generally increasing proton flux, with a superimposed solar-cycle modulation, as seen in the POES data, is also evident in the model results, except prior to about 1992 when a general increase is not predicted by the model.

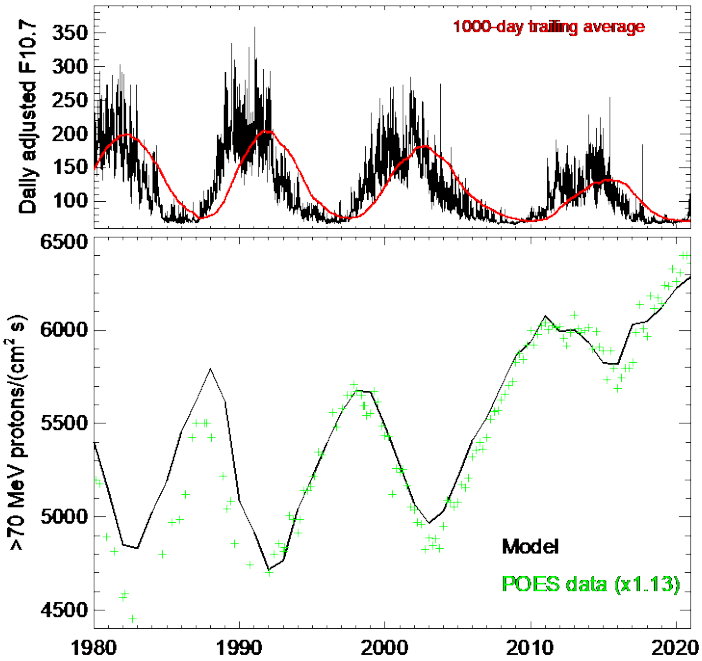

Figure 5. (Top) Daily adjusted F10.7 (black) and 1000-day trailing average of F10.7 (red); (Bottom) Model results for omnidirectional >70 MeV proton flux in the SAA at POES altitude at L=1.3 (black). POES flux was multiplied by a factor of 1.13 (green) for ease of comparison with the model.

At the low (~800 km) POES altitude, the model proton flux results mainly from a balance between the CRAND source and energy loss caused by atmospheric drag. The balance is established, at this altitude, after a model run of a few decades and no initial condition is therefore required. The rate of energy loss depends on upper atmospheric density, including neutral gas and plasma density, that increases with solar EUV input, as parameterized in the model by solar F10.7. Therefore, the trend of increasing SAA flux is a direct result, in the model, of the decreasing F10.7 values during successive recent solar maxima, as shown in Figure 1. The phase lag from F10.7 maxima to proton flux minima, of ~500 days in both the model and observations, results from the average time scale of proton energy loss at this altitude.

The model also predicts that the maximum SAA proton flux is near L=1.3 for > 70 MeV protons, as observed. However, this result is somewhat dependent on other model inputs, such as values

of the radial diffusion coefficient and an additional, unspecified loss process, with a mean lifetime of 22 years, that was added to the model by Selesnick and Albert (2019) to match observed radiation belt flux values. These factors have only a minor influence on model results near L=1.3, but do change the results at higher L and therefore influence the location of the flux maximum.

Similar model flux values (black line) across the first two solar cycles in Figure 5 result from similar corresponding F10.7 values. It is therefore unclear why the measured proton flux (green) showed generally increasing levels during this early period as well. A discrepancy between F10.7 and solar EUV flux during this period is possible or some other uncertainty in the model. However, generally similar time dependencies and absolute flux values in the data and model add confidence to the data interpretation over the forty year time scale shown.

5 Discussion and Conclusions

In general terms, the basic equation which balances thermal kinetic energy causing the atmosphere to expand against gravity pulling it earthward is (see Russell et al., 2016):

$n = n_0 \exp(-h/H)$

where h is altitude and $H = kT/mg$ is the scale length over which thermal pressure decays exponentially at a given fixed temperature T. This equation of hydrostatic equilibrium states that the scale height is longer therefore the atmosphere decays more slowly with h when T is greater. This explains the basic physics of why the loss rate of inner zone protons is lower when there is less solar energy input to the atmosphere. The lag time between solar minimum as measured by F10.7 and peak proton flux corresponds to the thermal intertia of the atmosphere. Selesnick et al. (2007) used the NRLMSISE-00 atmosphere model to calculate trapped proton flux in an IGRF magnetic field model. Their Figure 11 shows the altitude profile for two sample neutrals (H and N2) at different F10.7. When F10.7 increases from 60 to 220, the dominant N2 concentration increases at each altitude. This is due to increased EUV heating of the atmosphere for which F10.7 serves as a proxy. When F10.7 is not as high on average, as was the case for the recent solar maximum compared with prior maxima shown in **Figure 1**, there will be less N2 at a given altitude affecting collisional energy loss of protons. Figure 12 in Selesnick et al. (2007) shows that H^+, He^+ and O^+ density decreases at a given altitude as F10.7 decreases. The inner zone protons lose energy primarily via Coulomb collisions with both free and bound electrons (Selesnick et al., 2007; Selesnick and Albert, 2019), explaining the higher flux levels above a fixed energy following weaker solar maxima.

The Solar Cycle 24 flux minimum (December, 2015), averaged over the three energy channels studied, was calculated to be 19% higher than the Solar Cycle 23 minimum (October, 2002) (**Fig. 3**). The weaker Solar Cycle 24 solar maximum caused less atmospheric and ionospheric heating, thereby reducing inner zone proton energy loss via collisions and flux for the > 70 MeV energy channel shown in **Figures 1** and **2**. We found a similar trend in the >35 MeV and >140 MeV energy channels (**Fig. 3**). The flux increased from a high flux minimum in 2016 compared to prior minima since 1980 shown in **Figure 1**, to its highest maximum for the time period 1980 - 2021 examined by June 2021 .

While the short term variation within a solar cycle leading to higher flux lagging solar minimum is explained by the F10.7 variation within a solar cycle (Qin et al., 2014; Li et al., 2020; Lin et al., 2020), the longer term trend for >70 MeV protons seen in **Figure 1**, also evident but not noted by Qin et al. who examined NOAA POES flux at > 70 MeV from 1980 – 2010, requires consideration of longer term solar variations, notably the Gleissberg cycle (Gleissberg, 1965; Svalgaard et al., 2005; Feynman & Ruzmaikin, 2011, Pulkinnen et al., 2001). Feynman & Ruzmaikin (2011) described the Centennial Gleissberg Cycle as an approximately century-long sinusoidal variation in the intensity of solar maximum and found evidence to suggest that Solar Cycles 23 and 24 represent the minimum of this 80 to 100-year cycle. The onset of this Gleissberg cycle minimum in solar activity indicates that the increasing proton flux discussed in this paper is to be expected and serves to explain these results.

Note that Lin et al., (2020) recalibrated POES and MetOp satellite data using POES NOAA-15 as the reference standard but did not find a long-term increase in >16 MeV proton flux at constant L = 1.2. We focused on the three higher energy channels of POES energetic proton measurements: >35 MeV, >70 MeV and >140 MeV where electron contamination issues are known to be less significant (Janet Green, private communication). It was found that both the peak flux in the SAA and the flux at constant L=1.3 show the same long term trend. Further comparison with measurements from other spacecraft such as Van Allen Probes (Li et al., 2020) is warranted, including standardization of integral flux measurements across the POES data set when compared with measurements from the Relativistic Electron Proton Telescope on Van Allen Probes (Baker et al., 2013). However, the great value of the POES data set going back to 1980 is the unique long baseline used in the present study to identify the flux increase correlation with reduced solar activity over four solar cycles. From a space weather hazard standpoint, this long term increase in the flux of inner zone protons should be included in updated models of the space radiation environment.

Acknowledgments

This study is supported by AFOSR grant FA9550-20-1-0339. E.B. acknowledges support from the High Altitude Observatory Visitor Program, NCAR. We thank Drs. Janet Green, Rob Redmon, and Juan Rodriguez for discussion of the POES data.

Data Availability Statement

F10.7 data come from the OMNI database: https://omniweb.gsfc.nasa.gov/form/dx1.html. The data for POES are available at https://satdat.ngdc.noaa.gov/sem/poes/data/.

References

Baker, D. N., et al. (2013), The Relativistic Electron-Proton Telescope (REPT) Instrument on Board the Radiation Belt Storm Probes (RBSP) Spacecraft: Characterization of Earth's Radiation Belt High-Energy Particle Populations, *Space Sci. Rev.*, 179, 337– 381, doi:10.1007/s11214-012-9950-9

Cook, W. R., Cummings, A. C., Cummings, J. R., Garrard, T. L., Kecman, B., Mewaldt, R. A., Selesnick, R. S., Stone, E. C., Baker, D. N., von Rosenvinge, T. T., Blake, J. B., & Callis, L. B. (1993). PET: A proton/electron telescope for studies of magnetospheric, solar, and galactic particles. *IEEE Transactions on Geoscience and Remote Sensing*, 31(3), 565– 571. https://doi.org/10.1109/36.225523

Dragt, A. J. (1971), Solar cycle modulation of the radiation belt proton flux, *J. Geophys. Res.*, *76*(10), 2313–2344.

Dyer, C. (2002), Radiation effects on spacecraft and aircraft, in Proceedings of the Second Solar Cycle and Space Weather Euroconference, edited by H. Sawaya-Lacoste, Eur. Space Agency Spec. Publ., ESA SP-477, 505 -- 512.

Evans, D.S., and M.S. Greer (2006), Polar orbiting environmental satellite space environment monitor-2: Instrument descriptions and archive data documentation, *NOAA Techincal Memorandum, Boulder, Colorado OAR SEC 93, 93, version 2.0, 2006, https://satdat.ngdc.noaa.gov/sem/poes/docs/sem2_docs/2006/SEM2v2.0.pdf* .

Feynman, J., & Ruzmaikin, A. (2011). The sun's strange behavior: Maunder minimum or Gleissberg cycle? *Solar Physics*, *272*(2), 351–363. https://doi.org/10.1007/s11207-011-9828-0

Ginet, Gregory & O'Brien, T. & Huston, S. & Johnston, W. & Guild, Timothy & Friedel, R. & Lindstrom, C. & Roth, Christopher & Whelan, P. & Quinn, R. & Madden, D. & Morley, Steven & Su, Yi-Jiun (2013). AE9, AP9 and SPM: New Models for Specifying the Trapped Energetic Particle and Space Plasma Environment. Space Science Reviews. 179. 10.1007/s11214-013-9964y.

Gleissberg, W. (1965), The eighty-year solar cycle in auroral frequency numbers. J. Br. Astron. Assoc. 75, 227 – 231.

Gombosi T., Physics of the Space Environment (1998), Cambridge University Press, Cambridge, UK, doi:10.1017/CBO9780511529474

Huston, S., G. Kuck, and K. Pfitzer (1998), Solar cycle variation of the low-altitude trapped proton flux, *Adv. Space Res.*, *21*(12), 1625–1634.

Kuznetsov, N. V., N. I. Nikolaeva, and M. I. Panasyuk (2010), Variation of the trapped proton flux in the inner radiation belt of the Earth asa function of solar activity, *Cosmic Res.*, *48*(1), 80–85.

Li, X., Xiang, Z., Zhang, K., Khoo, L., Zhao, H., Baker, D. N., & Temerin, M. A. (2020). New insights from long-term measurements of inner belt protons (10s of MeV) by SAMPEX, POES, Van Allen probes, and simulation results. *Journal of Geophysical Research: Space Physics*, *125*(8). https://doi.org/10.1029/2020JA028198

Lin, R., Zhang, J., Zhang, X., Ni, B., Liu, S., Shi, L., et al. (2020). Long-term variations of >16-MeV proton fluxes: Measurements from NOAA POES and EUMETSAT MetOp satellites.

Journal of Geophysical Research: Space Physics, 125, e2019JA027635. https://doi.org/10.1029/2019JA027635

Nakano, G., and H. Heckman (1968), Evidence for solar-cycle changes in the inner-belt protons, *Phys. Rev. Lett.*, *20*(15), 806–809.

Pavón-Carrasco, F. J., & De Santis, A. (2016). The South Atlantic Anomaly: The key for a possible geomagnetic reversal. Frontiers in Earth Science, 4, 40.

Pulkkinen, TI, H Nevanlinna, PJ Pulkkinen, M Lockwood (2001), The Sun–Earth connection in time scales from years to decades and centuries, Space Science Reviews 95 (1), 625-637, https://doi.org/10.1023/A:1005299314802.

Qin, M., Zhang, X., Ni, B., Song, H., Zou, H., & Sun, Y. (2014). Solar cycle variations of trapped proton flux in the inner radiation belt. *Journal of Geophysical Research: Space Physics*, *119*(12), 9658–9669. https://doi.org/10.1002/2014JA020300

Rabin, V. J., D. S. Evans, H. H. Sauer, S. R. Sahm and M. Huynh (1995), TIROS/NOAA Satellite Space Environment Data Archive Documentation: 1995 Update, *NOAA Techincal Memorandum, ERL SEL -86, Boulder, Colorado, https://satdat.ngdc.noaa.gov/sem/poes/docs/sem1_docs/TIROS-NOAA_SEM_Data_Archive_Documentation_1995-update.pdf*

Reames, D., Ng, C., & Tylka, A. (1999). Energy-dependent ionization states of shock-accelerated particles in the solar corona. Geophysical Research Letters, 26, 3585–3588. https://doi.org/10.1029/1999GL003656

Russell, C. T., J. G. Luhmann, R. J. Strangeway (2016), Space Physics: An Introduction, Cambridge University Press, ISBN1107098823, 9781107098824

Selesnick, R. S., & Albert, J. M. (2019). Variability of the proton radiation belt. *Journal of Geophysical Research: Space Physics*, *124*(7), 5516–5527. https://doi.org/10.1029/2019JA026754

Selesnick, R. S., D. N. Baker, A. N. Jaynes, X. Li, S. G. Kanekal, M. K. Hudson, and B. T. Kress (2014), Observations of the inner radiation belt: CRAND and trapped solar protons, *J. Geophys. Res. Space Physics*, *119*, 6541–6552, doi:10.1002/2014JA020188.

Selesnick, R. S., Looper, M. D., & Mewaldt, R. A. (2007). A theoretical model of the inner proton radiation belt. *Space Weather*, *5*(4), n/a-n/a. https://doi.org/10.1029/2006SW000275

Selesnick, R. S., Hudson, M. K., & Kress, B. T. (2010). Injection and loss of inner radiation belt protons during solar proton events and magnetic storms. *Journal of Geophysical Research: Space Physics*, *115*(A8), n/a-n/a. https://doi.org/10.1029/2010JA015247

Singer, S. F. (1958), Trapped albedo theory of the radiation belt, Phys. Rev. Lett., 1, 181-- 183.

Stassinopoulos, E. G., & Raymond, J. P. (1988). The space radiation environment for electronics. *Proceedings of the IEEE*, *76*(11), 1423–1442. https://doi.org/10.1109/5.90113

Svalgaard, L., Cliver, E.W. and Kamide, Y. (2005), Sunspot cycle 24: Smallest cycle in 100 years? *Geophys. Res. Lett.*, 32, L01104, doi:10.1029/2004GL021664

Thébault,E. et al. (2015), International Geomagnetic Reference Field: the 12th generation. *Earth Planets Space* 67,79.doi:10.1186/s40623-015-0228-9

Van Allen, J. A., Ludwig, G. H., Ray, E. C., & McIlwain, C. E. (1958). Observation of high intensity radiation by satellites 1958 Alpha and Gamma. Journal of Jet Propulsion, 28, 588–592.Van Allen, J. A., Ludwig, G. H., Ray, E. C., & McIlwain, C. E. (1958).

Yermolaev, Y. I., Lodkina, I. G., Khokhlachev, A. A., Yermolaev, M. Yu., Riazantseva, M. O., Rakhmanova, L. S., Borodkova, N. L., Sapunova, O. V., & Moskaleva, A. V. (2021). Drop of solar wind at the end of the 20th century. *Journal of Geophysical Research: Space Physics*, *126*(9). https://doi.org/10.1029/2021JA029618